Charge transfer in low-energy collisions of He^{2+} with atomic hydrogen

C. C. Havener,* R. Rejoub, and P. S. Krstić
Physics Division, Oak Ridge National Laboratory, Oak Ridge, Tennessee 37831, USA

A. C. H. Smith
Department of Physics & Astronomy, University College London, London, WC1E 6BT, United Kingdom
(Received 4 June 2004; published 19 April 2005)

Using the Oak Ridge National Laboratory ion-atom merged-beams apparatus, absolute total charge-transfer cross sections have been measured for collisions of $He^{2+}+H$ over a range of energies from 380 to 2620 eV/u. The experimental results are compared to previous measurements using different experimental techniques. A hidden-crossing coupled-channel (HCCC) calculation is performed in the collision energy range of 10 to 3000 eV/u and is compared with the measured data as well as with other theories. The HCCC calculation, which is deemed accurate below 1000 eV/u, is also used to determine differential cross sections. The resultant angular scattering information is used to correct the merged-beams data, which is characterized by a large but limited angular acceptance at these collision energies. Our combined experimental and theoretical study provides an improved benchmark for this fundamental system.

DOI: 10.1103/PhysRevA.71.042707 PACS number(s): 34.70.+e

I. INTRODUCTION

Atomic hydrogen and helium are the most abundant elements in both astrophysical and terrestrial fusion plasmas. The charge-transfer (CT) reaction

$$He^{2+} + X \rightarrow He^{+*} + X^{+}, \tag{1}$$

where an asterisk represents any state of the He^+ product and X represents almost any neutral species, is highly relevant in the analysis of the near-edge region of fusion plasmas and in the study of the exhaust of the helium product from the fusion reaction. When X is atomic hydrogen in the ground state, the charge transfer process has a zero-energy defect for capture into the $n=2$ states of He^+. However, as first pointed out by Fite *et al.* [1], the energy defect at the internuclear separation where the electron transfer takes place is large because of the Coulomb repulsion of the charged products. Consequently, the cross section attains a peak value of 12×10^{-16} cm^{-2} at a collision energy around 10 keV/u and then, characteristic of "tunneling" through a potential barrier, the cross section exponentially decreases toward lower energies. This decreasing cross section along with inherent difficulties in producing a ground-state atomic hydrogen target makes low-energy measurements [1–6] difficult. In fact, the only total cross-section measurements below 1 keV/u are from early work of Fite *et al.* [1] and Nutt *et al.* [5]. Such total cross-section measurements using a tungsten tube furnace to produce H from H_2 require the fraction of dissociation and the H target number density to be accurately determined. The measurements of Fite *et al.* exhibit an approximately constant cross section value of 2.5×10^{-16} cm^{-2} as the energy is decreased below 1000 eV/u, whereas the later measurements of Nutt *et al.* show a rapid decrease below 1000 eV/u, more in line with the expected decrease of the cross section.

Due to a relatively small number of atomic states effectively involved in the charge-transfer process at low energies, $He^{2+}+H$ is one of the most-frequently theoretically studied collision processes and is viewed as a prototype one-electron heavy-particle, asymmetric collision system. An important advantage of studying single-electron, two-center systems is the availability of accurate adiabatic potential curves and wave functions. Due to the system separability in elliptic prolate coordinates, the adiabatic, quasimolecular, and electronic eigenenergies and eigenfunctions can be obtained with any desired accuracy, for arbitrary internuclear distance R [7]. These constitute the so-called molecular orbital (MO) basis for the molecular-orbital coupled-channel (MOCC) method, which is a usual method of choice for low energies (collision velocity $v \ll v_0$, where v_0 is the characteristic electron velocity in the initial state).

Despite numerous theoretical works in the last few decades [8–26] on $He^{2+}+H$, the calculated CT data are still neither fully consistent with each other nor with experiments at low collision energies. There are several reasons for the disagreement, depending on the considered subrange of energies. For example, below about 400 eV/u, a classical trajectory treatment of internuclear motion is inadequate, as already pointed by Winter and Lane [9] in the late 1970s. A straight-line trajectory leads in the MOCC method to an overestimation of the cross section, providing more charge transfer from united-atom (UA) rotational coupling of the initial $2p\sigma$ with $2p\pi$ quasimolecular states (in the notation of the UA spherical quantum numbers) than is "allowed" by nuclear repulsion [23]. Even with a fully quantum treatment of nuclear motion the various sources in the literature [9,13,18,26,27] report cross sections that disagree by orders of magnitude at lower energies. Significant progress toward mutual concordance of various methods at low energies has recently been reported by Krstić [27] and Lin and co-workers [28]. Above a few hundreds of eV/u the dispersion of re-

*Electronic address: havenercc@ornl.gov

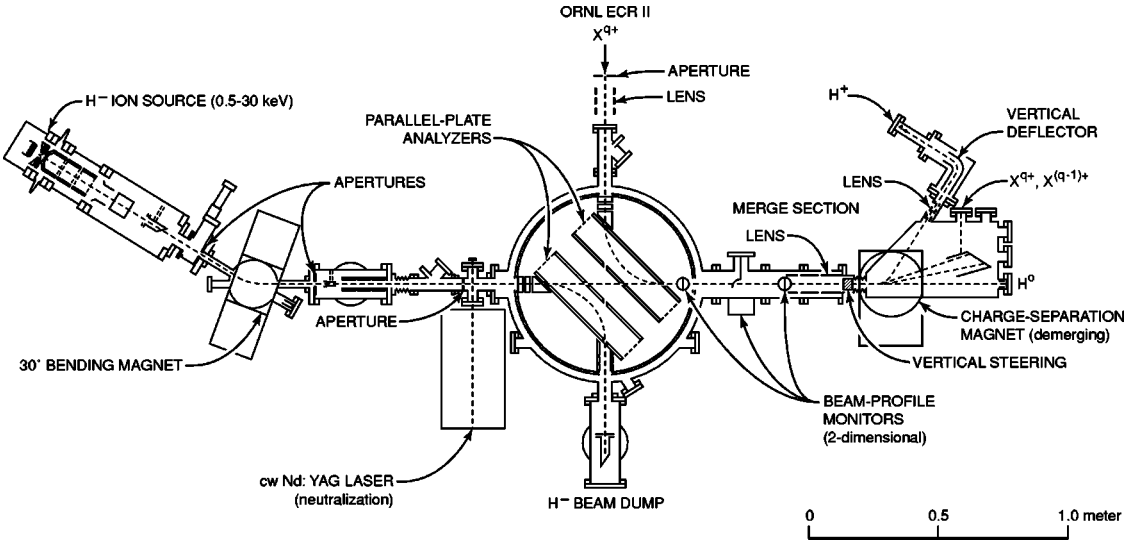

FIG. 1. Schematic of the ion-atom merged-beams apparatus.

ported theoretical data decreases, nevertheless staying within 50%. Such a large uncertainty is caused by the need for a larger and larger MO basis for convergence with increasing energy, as well as by the diversity of electron translation factors (ETF) used to cure the problems inherent to the MOCC method (boundary conditions of the nonadiabatic matrix elements, size inconsistency of a truncated molecular basis).

In view of the continued attention and importance of this fundamental system, further experimental and theoretical studies are needed to establish an improved benchmark. The merged-beams technique [29] described in Sec. II is fundamentally different from the previous experiments and provides a truly independent measurement of the total charge-transfer cross section for $He^{2+}+H$. The calculation, performed earlier [27] by the hidden-crossing coupled-channel (HCCC) method [27,30,31] for the $He^{2+}+H$ charge transfer at low energies, is described and extended up to 3 keV/u in Sec. III to compare with the measured data. An analysis, discussion, and comparison of our measured and theoretical data, mutually and with those available in the literature, are presented in Sec. IV. Finally, our concluding remarks and summary are given in Sec. V.

II. EXPERIMENT

The measurement of the charge-transfer cross section for the $He^{2+}+H$ system was performed at the Multicharged Ion Research Facility (MIRF) at Oak Ridge National Laboratory (ORNL) using the ion-atom merged-beams apparatus, which has previously been described in detail [29,32]. The apparatus, shown schematically in Fig. 1, has been highly successful in providing benchmark CT total cross sections [33] for a variety of multiply charged ions in collisions with H and D. In the merged-beams technique used here, relatively fast (keV) ion and atomic beams are merged, producing a large dynamic range of possible center-of-mass (c.m.) collision energies, from keV/u down to meV/u. In the present investigation, a $^3He^{2+}$ beam with energies of 17–25 keV was merged with a fast H beam with energies of 6, 8, and 9 keV. This range of primary beam energies permitted the total charge-transfer cross section to be measured over the energy range of 380–2620 eV/u. A fast neutral ground-state hydrogen beam is obtained by photodetachment of a H^- beam as it crosses the optical cavity of a 1.06-μm cw Nd:YAG laser where kilowatts of continuous power circulate. The H^- is extracted from a duoplasmatron ion source. Collisional detachment of the H^- beam in the background gas results in a small fraction (0.01%) of excited-state contamination in the H beam. The H beam is highly collimated (the divergence is less than 0.15°), with a beam diameter of 2 mm and intensities ranging from 20 to 40 nA.

As depicted in Fig. 1, the He^{2+} beam is electrostatically merged with the neutral H beam. A 4–10-μA He^{2+} beam is produced by the ORNL Caprice ECR ion source with a diameter of 3 mm [full width at half maximum (FWHM)] and a divergence less than 0.25°. The two beams interact along a field free region of 47 cm, after which H^+ product ions are magnetically separated from the primary beams. The neutral beam is monitored by measuring secondary-electron emission from a stainless-steel plate, and the intensity of He^{2+} beam is measured by a Faraday cup. The product signal of H^+ ions is detected with a channel electron multiplier operated in pulse-counting mode. The beam-beam signal rate (Hz) is extracted from the (kHz) background with a two-beam modulation technique. The dominant background arises from H stripping on residual gas. To correct the beam-beam signal rate for the small fraction of excited H, the signal is measured with and without the laser on. The difference between the signals corresponds to the ground-state collisions.

The absolute charge-transfer cross section is determined at each velocity from directly measurable parameters from the formula

$$\sigma = \frac{S\gamma q e^2 v_1 v_2}{I_1 I_2 v_r L \langle F \rangle}, \tag{2}$$

where S is the signal count rate, q is the charge number of the ion, e is the electronic charge, I_1 and I_2 are the currents of the beams, v_1 and v_2 are the velocities of the beams, v_r is the relative velocity of the beams, L is the merge-path length, γ is the secondary-electron emission coefficient of the neutral detector, and $\langle F \rangle$ is the average form factor measuring the overlap of the beams. The form factor is estimated from two-dimensional measurements of the beam-beam overlap at three different positions along the merged path. The secondary-electron emission coefficient γ is measured *in situ* as described previously [32]. The velocities are calculated from the accelerating voltages of the beams, which include the estimated plasma potential shifts of the two sources (see, e.g., Ref. [34]). The effect of the small (nonzero) angle between the merged beams was found to be negligible in the range of cm collision energies reported here.

In this (single-pass) merged-beams experiment, the target density of the H beam [29] is several orders of magnitude less than for an H target formed from dissociation of H_2. This makes the merged-beams measurements difficult, especially when the cross section is below 10^{-16} cm^2. The lowest energy at which measurements can be performed is determined by the inherent signal/noise ratio. The signal/noise ratio degrades toward lower energies due to a decreasing number of collisions in the merge path (the number of beam-beam collisions is proportional to the relative collision velocity [29]), a decreasing cross section, and a large constant background (10–20 kHz). The unusually large background is due to collisions of H with the $\sim 10^{-9}$ Torr He background gas in the merge path. The high He partial pressure is a result of depositing the microampere intensity He beam in the collision chamber and the relatively low He pumping capacities in cryogenic pumps. The signal/noise ratio is reflected in the statistical error reported for each measurement.

Low-energy charge-transfer collisions can exhibit significant angular scattering in the center-of-mass frame [35]. However, because of the kinematic frame transformation, this angular scattering is significantly compressed in the laboratory frame, the frame in which the products are collected. The angular acceptance of the the ORNL merged-beams apparatus in the laboratory frame was determined to be at least 2.3°, as determined by ray tracings and verified by comparison of data to angular-scattering calculations for the O^{5+} system (see Refs. [36,37]). From this estimate, one can determine the maximum angle into which the product H^+ can be emitted in the center-of-mass frame and still be collected. Figure 2 shows the angular acceptance in the center-of-mass frame in the forward direction as a function of collision energy for capture into the $n=2$ level of He^+ using a 9.068 keV H beam. For scattering in the backward direction the angular acceptance is similar, because only the velocity component perpendicular to the beam direction leads to a loss of signal. Figure 2 shows that the angular acceptance improves with decreasing collision energy. Though not relevant to this system, there is usually an energy ($\sim$10 eV/u) below which all products are collected. Comparison of the angular acceptance to the angular scattering calculations will determine whether all products are collected (see Sec. IV).

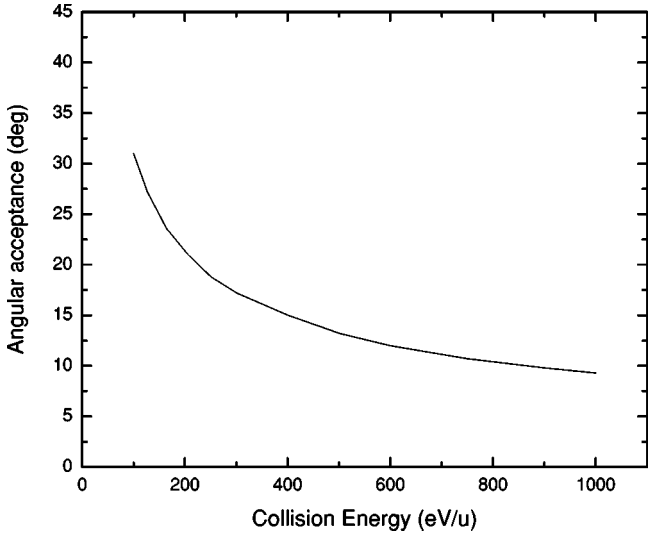

FIG. 2. Current angular acceptance of the ORNL ion-atom merged-beams apparatus in the forward direction in the center-of-mass frame as a function of collision energy for measurements in the $He^{2+}+H$ system performed with a 9.068-keV H beam.

III. THEORY

Knowledge of accurate potential surfaces in the plane of complex internuclear distance, R, encouraged recent development of an advanced adiabatic theory of collisions, known as the hidden crossing theory [19,38–41]. Although the treatment of the collision dynamics in the HC theory varies with the specific approach, common to all of them is use of the topology of the adiabatic eigenenergy surfaces in the plane of complex R, which is assumed to contain all information on the radial transition dynamics in the low-collision-velocity limit. Qualitative understanding of the collision dynamics from topology is one of the highlights of the HC theory and is summarized below. More details on the topology of the studied system can be found in a previous publication [19].

Figure 3(a) shows the adiabatic quasimolecular electronic eigenenergies for $(HeH)^{2+}$ of the states used in the current calculation ($N_{\rm eff}=\sqrt{Z^2/2|E_N|}, Z=3$). Being interested in charge transfer from the ground H(1s) state (corresponding to the $2p\sigma$ molecular state), only 12 of the lowest states that can be reached in at most two consecutive state-to-state steps along a transition path are taken into account in either the incoming or receding collision phase, in any combination of the radial and rotational transitions. An exception is $5g\sigma$, which requires three subsequent transitions and is kept here as one of the states of the excited H($n=2$) multiplet. Figure 3(b) shows the most important (single-step) transitions from the ground state.

As discussed in the Introduction, the rotational coupling $2p\sigma$-$2p\pi$ has a leading role in the charge-transfer process below about 400 eV/u, but its role diminishes below 60 eV/u, because of nuclear repulsion. Also the role of the

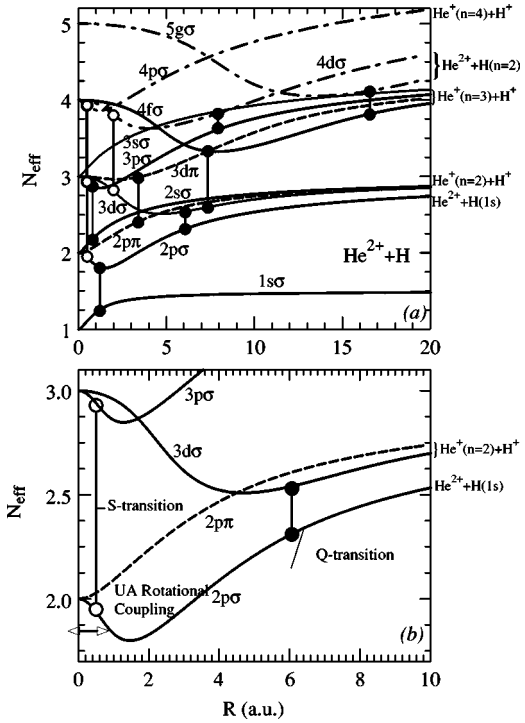

FIG. 3. Adiabatic quasimolecular electronic eigenenergies as a function of internuclear separation for $(HeH)^{2+}$. See text for details. (a) shows all states used in the calculation.(b) shows the most important (single-step) transitions from the initial ground state of $He^{2+}+H(1s)$.

radial transitions, symbolically presented in Fig. 3 with circle-line-circle symbols (solid circles denote *Q* series, open circles denote *S* series [19]), as well as the UA rotational coupling of the $3p\sigma$-$3p\pi$ and $3d\sigma$-$3d\pi$-$3d\delta$ states, gradually increases with increasing energy. With a new hidden-crossing coupled-channel approach, performing calculations with 3, 8, and 12 states, convergence is reached for the total cross section to better than three digits of accuracy in the whole considered energy range 10–3000 eV/u.

The correct application of the HC theory in the nearly adiabatic limit depends on the description of the collision dynamics in that limit. The recent advancement in HC theory, the HCCC method [30,31], looks similar to the standard fully quantal MOCC method, but as a significant difference, the nonadiabatic matrix elements $U_{ij}(R)$ are defined utilizing the hidden-crossing topology. The first approximation beyond the assumption of the complete localization of the transition (which is exact only, in the strict adiabatic limit) around the real part of the complex crossing radius, $\mathrm{Re}\{R_c\}$ [30], is the linear expansion in complex R around R_c of the relevant interacting-state parameters, which leads to a Lorentzian model for the nonadiabatic coupling [30]:

$$U_{ij}(R) = \langle \varphi_i | \partial/\partial R | \varphi_j \rangle = \frac{1}{2} \frac{\mathrm{Im}\{R_c\}}{(R - \mathrm{Re}\{R_c\})^2 + (\mathrm{Im}\{R_c\})^2}. \quad (3)$$

A U_{ij} defined thus does not suffer from the problems of the standard MOCC method: it complies with the boundary conditions—i.e., $U_{ij}(R\to\infty)\to 0$—and it is not dependent on the choice of the electronic origin, thus enabling reliable results with a small number of states. The Lorentzian behavior of the matrix elements is accurate only in the vicinity of $\mathrm{Re}\{R_c\}$ when $v\to 0$ (a consequence of the transition localization) while the fast oscillating dynamic phase of the interacting states (proportional to their energy splitting and $1/v$) suppresses possible spurious transitions far from $\mathrm{Re}\{R_c\}$. Exceptions are the radial terms which are degenerate when $R\to\infty$ and correspond to the eigenfunctions localized at the different centers. Decrease of the relevant $U_{ij}(R\to\infty)$ as $1/R^2$ (rather than exponentially) can significantly and falsely influence the CT results at low energies (below 60 eV/u for the considered system). This is resolved elsewhere [27] in a self-consistent manner, by applying a functional multiplier at $U_{ij}(R)$ in Eq. (3), which decreases faster than $1/R^2$ far from $\mathrm{Re}\{R_c\}$, while simultaneously maintaining $U_{ij}(R)$ in its vicinity. The applicability of the HCCC method is limited at higher velocities, in the keV region, and is usually handled in the HC theory [19,40,41] by truncation of the partial-wave contributions to the cross sections at $\ell_{\max}=k|R_c|+2/v$ [41]—i.e., at $b_{\max}=|R_c|$ in the impact parameter formalism. For the collision system studied here the truncation is applied above $E=750$ eV/u and the cross section is calculated as $\sigma(E)=\Sigma^{\ell\max}\sigma_\ell(E)$, where the partial cross section [labeled as PCS in Fig. 4(a)] $\sigma_\ell(E)=(\pi/k^2)(2\ell+1)P_\ell(E)$ and $P_\ell(E)$ is the total transition probability for the charge transfer. Figure 4(a) shows $\sigma_\ell(E)$ for the energies of $E=250$ eV/u and, Fig. 4(b), $bP(b)$ for $E=750$ eV/u ($b=l/k$) (lines) and their comparison with hyperspherical coupled channel calculations (HSCC's) of Lin and co-workers [26,28] (symbols). The agreement of the partial cross sections is excellent at 250 eV/u, but deteriorates at 750 eV/u, with obvious slow decay of $bP(b)$ toward larger b. The agreement of the total cross section with the one obtained by HSCC's at $E=2000$ eV/u is also very good, while at 750 eV/u the two values deviate by 15%. The small-ℓ peak at 250 eV/u emerges from the UA $2p\sigma$-$2p\pi$ rotational coupling, while the oscillatory part of the curve is from the $2p\sigma$-$3d\sigma$ radial coupling (see Fig. 3). Since HSCC's do not make any assumptions on the UA rotational coupling approximation, Fig. 4(a) confirms the effectiveness of the chosen approximation for the rotational couplings in the HCCC approach. The agreement of the HCCC and HSCC partial cross sections is even better with decreasing collision energy. The two sets of total cross-section data deviate by less than 5% at energies below 250 eV, down to 20 eV/u [27]. Although the HCCC method is asymptotically exact in the adiabatic limit ($v\to 0$), its accuracy toward higher energies depends on the system and processes considered. The need for truncation in the total cross-section calculations to $\ell_{\max}$ in the HCCC approach at higher energies (750 eV/u in this case) defines the higher limit in energy for its applicability as an independent and accurate method. Although the asymptotic nature of the method allows the possibility of obtaining accurate results at even higher energies, its accuracy can be estimated only by comparison with other theoretical and experimental data.

The HCCC method applied here uses a fully quantal MO method [42] by expanding the total scattering wave function in the sum of products of electronic adiabatic molecular

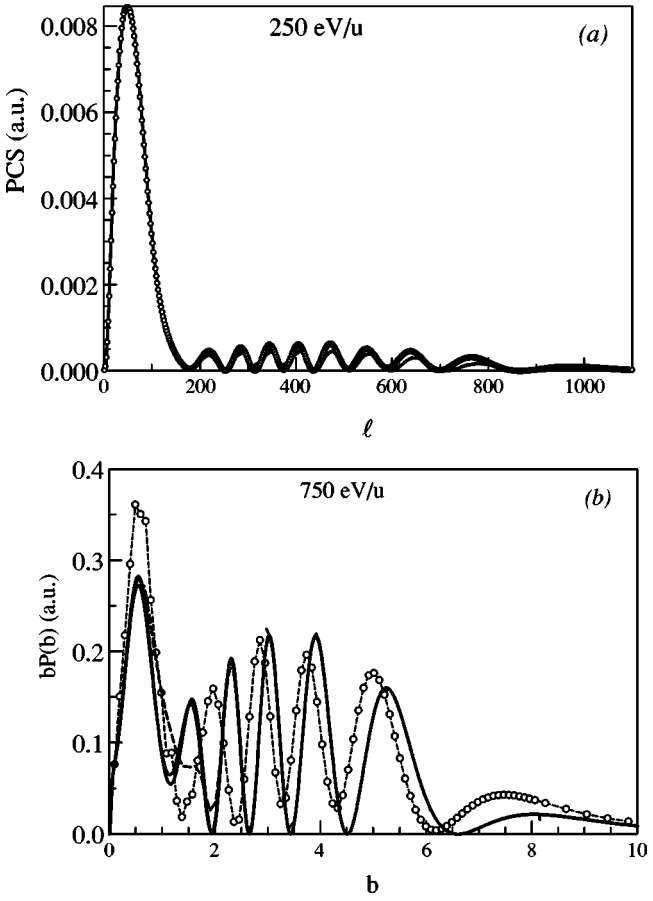

FIG. 4. Comparison of the present HCCC calculation with the hyperspherical coupled-channel calculations of Lin and co-workers [26,28]. (a) shows $\sigma_\ell(E)$ for an energy of $E=250$ eV/u (b) shows $bP(b)$ for $E=750$ eV/u. See text for details.

wave functions and nuclear wave functions. Using the matrix **U** of nonadiabatic radial matrix elements U_{ij} which are approximated by Eq. (3), at each of the hidden crossings between the chosen truncated set of adiabatic wave functions, the adiabatic electronic basis $\vec{\varphi}$ is transformed to the diabatic one $\vec{\varphi}^d$, such that $\langle\varphi_i^d|\partial/\partial R|\varphi_j^d\rangle=0$. This transformation and the numerical procedure are described in detail by Heil *et al.* [43]. The unitary transformation matrix $\mathbf{C}(R)$ is calculated numerically using $\mathbf{U}(R)$. The expansion of the total wave function in diabatic electronic functions is applied in the time-independent Schrödinger equation, obtaining a set of coupled second-order differential equations for nuclear functions $\vec{\mathbf{F}}^d(\vec{R})$:

$$\left(-\frac{1}{2M}\nabla_R^2\mathbf{I}-\mathbf{\Lambda}(R)+\varepsilon\mathbf{I}\right)\vec{\mathbf{F}}^{\mathbf{d}}(\vec{R})=0, \tag{4}$$

where M is the system reduced mass and **I** is the identity matrix. Upon expansion in partial waves, Eq. (4) is solved numerically in terms of the Johnson log-derivative method [44]. For the $He^{2+}+H$ system studied here, a step of $\Delta R=0.001$ is used and the integration starts from $R_{\min}=0.01$, while subject to the plane-wave boundary conditions at $R_{\max}=200$. Important for the present approach is that the

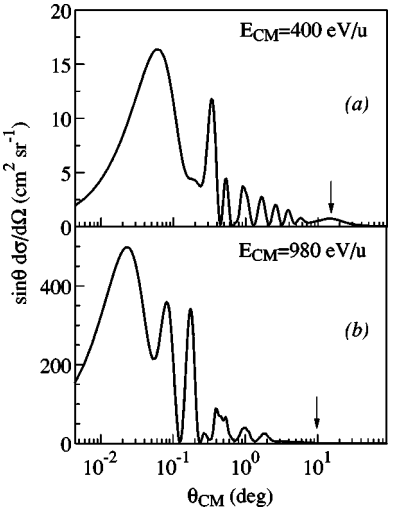

FIG. 5. Differential angular scattering versus center-of-mass angle calculated using the HCCC method for (a) 400 eV/u and (b) 980 eV/u collision energies. See text for details.

diabatic potential energy matrix $\mathbf{\Lambda}(R)=\mathbf{C}^{-1}(R)\mathbf{W}(R)\mathbf{C}(R)$, where $\mathbf{W}(R)$ is the diagonal adiabatic potential energy matrix, does not contain matrix elements of the second derivatives $(\partial^2/\partial R^2)$ which removes the need for additional approximations.

The resulting S matrix is used to calculate the charge-transfer probabilities and partial (in l), differential (in scattering angle), and total cross sections. Transitions between the scattering channels are induced by both radial and rotational nonadiabatic coupling matrix elements. The rotational matrix elements are defined in the usual way [42], where $\langle\varphi_i|iL_y|\varphi_j\rangle$ is approximated with a UA approximation. These are affected by transformation to the diabatic representation indirectly through the change of the relevant manifolds of radial states which are coupled by rotational coupling [45].

Figure 5 shows the calculated differential cross sections for collision energies of 400 and 980 eV/u. Especially at 400 eV/u two components can be observed: a forward-scattering component which can be associated with large impact parameter radial couplings (see Fig. 3) and a large angular-scattering component which is associated with the rotational coupling at smaller impact parameters. Backward scattering is found to be negligible at these energies. In both Figs. 5(a) and 5(b) an arrow indicates the angular acceptance of the present merged-beams apparatus in the center-of-mass frame. The integral of the differential cross section up to the angular acceptance in the center-of-mass frame is compared to the total cross section to determine the fraction of signal collected. The angular scattering calculations indicate that only 60% of the signal is collected at 400 eV/u while 97% is collected at 980 eV/u where the scattering is mostly forwardly peaked.

IV. RESULTS AND DISCUSSION

The present experimental results are tabulated in Table I. The cross section is multiplied by a correction factor to ac-

TABLE I. Measured ion-atom merged-beams cross section data for $He^{2+}+H \rightarrow He^{+}+H^{+}$ as a function of collision energy. Also listed is the statistical uncertainty and total combined (statistical plus systematic) uncertainty estimated at the 90% confidence level. See text for details.

Collision energy (keV/u)	Cross section (10^{-16} cm^2)	Statistical uncertainty (10^{-16} cm^2)	Total uncertainty (10^{-16} cm^2)
0.38	0.52	0.24	0.28
0.53	0.53	0.25	0.27
0.65	1.01	0.19	0.22
0.80	1.06	0.16	0.20
1.06	2.58	0.18	0.35
1.49	4.14	0.29	0.57
2.01	5.84	0.38	0.78
2.62	8.12	0.40	1.05

count for the predicted loss in signal due to angular scattering. The multiplicative factors at 0.38, 0.53, 0.65, 0.8, and 1.06 keV/u are 1.64, 1.27, 1.12, 1.06, and 1.03, respectively. Corrections at higher energies are not significant. The cross section is given along with the relative (statistical) error at 90% confidence and with the absolute error at 90% confidence. The absolute error is a quadrature sum of the relative, the estimated systematic errors of 12% (see Ref. [32]), and an estimated 25% error in the correction factor. Figure 6 shows a comparison of the present measurements with the results of earlier experiments [1–5,46]. The pioneering work was performed by Fite *et al.* [1] in the early 1960s, using a tungsten tube furnace technique to measure the total charge exchange cross section from 30 eV/u to 12 keV/u. The cross section of Fite *et al.* in Fig. 6 is a renormalized one, done by Shah and Gilbody [2] using more accurate values of $H^{+}+H$ charge transfer, obtained by McClure [47]. Although the renormalized cross section of Fite *et al.* above 1 keV/u is in accord with the later measurements of other authors, it exhibits an approximately constant value of about 2×10^{-16} cm^2 at energies below 1 keV/u. The behavior at these lower energies is at odds with all later experimental and theoretical results, and, as discussed previously [5], besides other problems connected to the nonselective detection

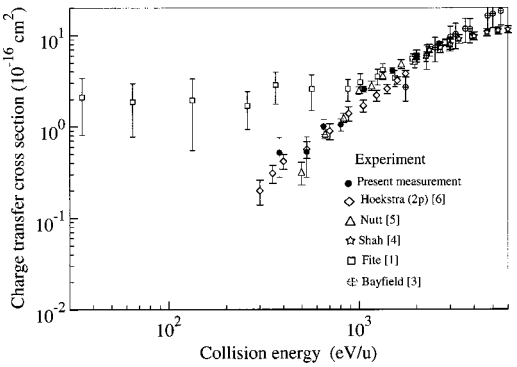

FIG. 6. The present total charge-transfer cross-section measurements for $He^{2+}+H$ compared to other total and state-selective ($2p$) measurements. The error bars of the present measurement represent relative errors at 90% confidence level. See text for details.

in the experiment of Fite *et al.* no correction was made for the effect of undissociated H_2 molecules in the target.

Shah and Gilbody [2,4] and Nutt *et al.* [5] modified the tungsten-tube furnace-target technique to provide a target with a higher fraction of dissociated hydrogen. The measurements of Nutt *et al.* extend toward lower energies, covering the range between 500 and 3000 eV/u. Our results extend to slightly lower energy and show good agreement with the measurements of Nutt *et al.* [5]. Total cross-section measurements using a tungsten-tube furnace to produce H from H_2—e.g., Nutt *et al.* [5]—require the fraction of dissociation and the H target number density to be determined. This is accomplished by normalization to other data and leads to systematic errors typically of 13% [5]. Accurate determination of the dissociation fraction is especially important for systems like this one where the cross section for H_2 is significantly different from the cross section for H. Reproducibility errors, as typified by the measurements of Nutt *et al.*, range from 7% at the high energies to 28% at the lowest energy of 497 eV/u. Investigation [48] of gas cell measurements by Nutt *et al.* [5] for collisions of He^{2+} ions with He and H_2 points to insufficient angular acceptance in some of the earlier measurements. Corrections have been applied to some of the previous data [48]. This may explain why the lowest energy point of Nutt *et al.* in Fig. 6 seems to be somewhat low.

Above 1 keV/u, our results show excellent agreement with Fite *et al.*, Shah and Gilbody, and Bayfield and Khayrallah [3] who measured the total charge-transfer cross section from 1.75 to 36.0 keV/u. At the highest collision energy of 2.62 keV/u our results are a few percent higher than the average value of Shah and Gilbody, Nutt *et al.*, and Bayfield and Khayrallah; however, the deviation is just outside the statistical error bars.

There also have been numerous state-selective cross-section measurements (see, e.g., [2–4,6,46,49,50] for the $He^{2+}+H$ system. Hoekstra *et al.* [6] measured the low-energy photon emission for $He(2p \rightarrow 1s)$ in the energy range 300–1750 eV/u (see Fig. 6) using a crossed-beam configuration with the H beam produced by a radio-frequency source with a 55% dissociation of H_2. Systematic errors resulting from the determination of the target density and spec-

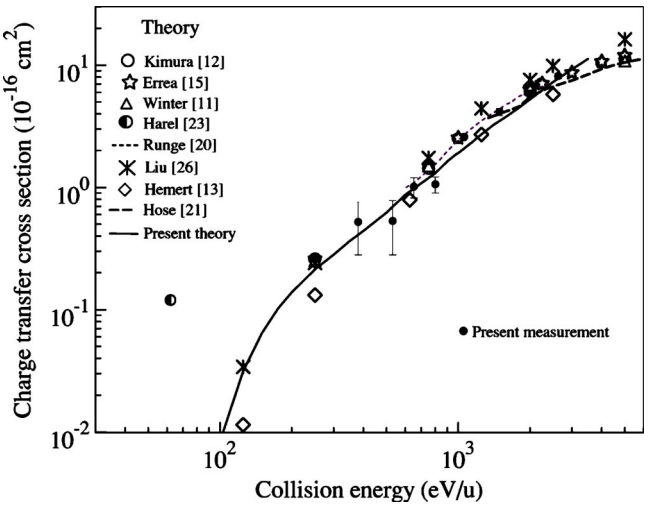

FIG. 7. The present total merged-beams measurements compared to the present HCCC calculations and to a selection of other theories. See text for details.

trometer calibration were 16% for $He(2p \rightarrow 1s)$ emission with reproducibility errors between 8% and 30%. The partial cross section can be associated with the total charge transfer at the lowest energies, since charge transfer to $He^+(2p)$ is the dominant process. As seen in Fig. 6, below 1 keV/u the $2p$ cross section is not observed to be significantly different from the present total cross-section values. However, above 1 keV/u the $2p$ cross section lies below the total cross-section values. This is expected, since the contribution of charge transfer to the subdominant $He^+(2s)$, as well as higher (n) states, becomes more significant [46], and additional emissions, including cascades, must be taken into account in order to fully describe the charge transfer.

To summarize the comparison of experiment, between 600 eV/u and 1 keV/u, the agreement between experiments is good enough to suggest that the total cross section is determined to better than 15% (including systematic errors) and, above 1 keV/u, where the statistical errors are negligible, to better than 10%. Below 600 eV/u the statistical errors are significant but the present measurements are consistent with the minimum total cross section provided by the $2p$ measurement of Hoekstra *et al.*, while the lowest-energy measurement of Nutt *et al.* is low.

Figure 7 compares the present merged-beams measurements to present HCCC calculations and some previous theoretical results. The four measured points at or below 800 eV/u show good agreement with the present calculation, the comparison being within or close to the statistical uncertainty of the measurement. In the energy range 1000–1500 eV/u our calculation underestimates the measured data by less than 20%, while in the interval 2000–2500 eV/u range the calculation agrees with the present measurements within the relative error.

Comparing the present measurement and calculation with previous theoretical data, agreement is obtained within the statistical uncertainties of the measurement in the range of from 1000 to about 2000 eV/u with the calculation of Runge and Micha [20], obtained by a semiclassical, eikonal time-dependent Hartree-Fock method, using a Gaussian basis of six hydrogenic orbitals and with ETF's. In the same energy interval the present calculation underestimates the Runge-Micha data by less than 20%, while above 2000 eV/u this disagreement drops below 10%. At lower energies (600–1000 eV/u) the Runge-Micha data are above the present calculation by up to 20% and even more so the measured data. Similar to the Runge-Micha results is the calculation of Kimura and Thorson [12], who used optimized non-common TF's, and of Winter and Haton [11] who used plane-wave (PW) ETF's. Errea *et al.* [14] calculated the cross section using the MOCC method with a common translational factor (CTF) approach, norm optimized [15], with a classical, straight-line trajectory, using ten states in the range 0.75–16 keV/u. Later calculations of Errea *et al.* were improved toward higher energies and included a larger MO basis [17] and ionization [22] using the triple-center MO basis. The calculations of Errea *et al.* are in good agreement with the data of Kimura and Thorson, Winter and Haton, and Runge and Micha for energies above 1000 eV/u as well as with those of Harel *et al.* [23], who also used CTF's and straight-line trajectories in a 66-state basis. The calculations of Harel *et al.* and Winter and Haton overestimate the present HCCC cross section by about 20% at 250 eV/u. The calculation of Harel *et al.* is orders of magnitude [27] higher at low energies (60 eV/u), which is, as discussed earlier, an arti-fact of the prescription of the straight-line trajectory. The MOCC-ETF data of van Hemert *et al.* [13] underestimate the present calculated data by about a factor of 3 at 125 eV/u, by 75% at 250 eV/u, and by 15% at 750 eV/u. At higher energies this calculation underestimates all other theoretical and experimental data. Hose [21] used the multichannel propagator technique with 45 adiabatic basis states, augmented with pseudoionization states in linear combination of Gaussian orbitals over a wide range of energies above 1350 eV/u. Although this calculation coincides with the Runge-Micha data at lower energies, it agrees with the present calculation in the interval 1800–2300 eV/u and then underestimates our calculation (20% at 3000 eV/u), coinciding with calculations of Kimura and Thorson, Errea *et al.*, and Winter and Haton at about 5000 eV/u. The Hose data agree well with the present measurement in the interval 1350–2600 eV/u, slightly underestimating it at the highest energies.

As previously discussed in Sec. III, Liu *et al.* and coworkers [26,28] have recently applied the hyperspherical close-coupling (HSCC) method to treat charge transfer for $He^{2+}+H$, in the range of c.m. collision energies from 10 eV/u to 4 keV/u. In their initial formulation [26], the calculation was performed within the manifold of four adiabatic hyperspherical states [the initial $H(1s)$ and the final $He^+(n=2)$ states]. Although this carefully performed, numerically intensive fully quantal calculation accounts well for all underlying physics below 200–300 eV/u, its accuracy must be judged at higher energies due to the limited adiabatic basis. Our previously reported HCCC calculation [27] for the lower-energy range showed an excellent agreement with the results of Liu *et al.* in the range 10–400 eV/u, which is within a few percent below 125 eV/u, rising to somewhat less than 10% at 250 eV/u. A similar agreement

with a fully quantal, distorted atomic-orbital calculations of Fukuda and Ishihara [18] for energies below 250 eV/u provides a confidence in the present theoretical data for energies below the range of the present experiment. At higher energies the data of Liu *et al.* overestimate our present experimental and theoretical results by over 50% at about 750 eV/u, reaching 60% at 1250 eV/u and staying over 40% for higher energies. Recently, the same authors performed the calculations with 10 and 20 hyperspherical adiabatic basis states. The new results [28] which are lower than their previous results [26] at higher energies still overestimate the present calculation at 750 eV/u by 20% (and somewhat more the measurement), but coincide with both the present calculation and experiment (within the statistical uncertainty) at 2000 eV/u.

V. SUMMARY

Absolute total charge-transfer cross sections for $He^{2+}+H$ have been measured using a merged-beams technique for collision energies from 380 to 2620 eV/u and compared to previous total and state-selective cross-section measurements. The hidden-crossing coupled-channel approach a variant of the MOCC method, has been extended from lower energies to the energy region of the experiment. A comparison with previous experimental and theoretical data was performed to analyze the current status and quality of the knowledge of charge transfer for this fundamental collision system. This combined experimental and theoretical study provides an improved benchmark for low-energy charge transfer. Below 600 eV/u our HCCC calculation provides the best estimate of the total cross section, while at higher energies, in particular above 1 keV/u, the calculated data cannot serve as an independent benchmark due to the low-energy asymptotic adiabatic nature of the HCCC method. Above 600 eV/u the present measurement shows excellent agreement with previous experiments, providing an improved benchmark for comparison with theory.

ACKNOWLEDGMENTS

This work was supported by the Division of Chemical Sciences, Office of Basic Energy Sciences, U.S. Department of Energy and (P.S.K.) by the Division of Applied Plasma Physics, Office of Fusion Energy Sciences, U.S. Department of Energy, Contract No. DE-AC05-00OR22725 with UT-Batelle, LLC, and (R.R.) by the NASA SARA program under Work Order No. 10,060 with UT-Batelle, LLC. One of the authors (R.R.) gratefully acknowledges the support from the ORNL Postdocoral Research Associates Program administered jointly by Oak Ridge Institute for Science and Education and Oak Ridge National Laboratory.

[1] W. L. Fite, A. C. H. Smith, and R. F. Stebbings, Proc. R. Soc. London, Ser. A **268**, 527 (1962).
[2] M. B. Shah and H. B. Gilbody, J. Phys. B **7**, 630 (1974).
[3] J. E. Bayfield and G. A. Khayrallah, Phys. Rev. A **12**, 869 (1975).
[4] M. B. Shah and H. B. Gilbody, J. Phys. B **11**, 121 (1978).
[5] W. L. Nutt, R. W. McCullough, K. Brady, M. B. Shah, and H. B. Gilbody, J. Phys. B **11**, 1457 (1978).
[6] R. Hoekstra, A. R. Schlatmann, F. J. De Heer, and R. Morgenstern, J. Phys. B **22**, L603 (1989).
[7] J. D. Power, Philos. Trans. R. Soc. London, Ser. A **274**, 663 (1973).
[8] R. D. Piacentini and A. Salin, J. Phys. B **7**, 1666 (1974).
[9] T. G. Winter and N. F. Lane, Phys. Rev. A **17**, 66 (1978).
[10] G. J. Haton, N. F. Lane, and T. G. Winter, J. Phys. B **12**, L571 (1979).
[11] T. G. Winter and G. J. Haton, Phys. Rev. A **21**, 793 (1980).
[12] M. Kimura and W. R. Thorson, Phys. Rev. A **24**, 3019 (1981).
[13] M. C. van Hemert, E. G. van Dishoeck, J. A. van der Hart, and F. Koike, Phys. Rev. A **31**, 2227 (1985).
[14] L. F. Errea, J. M. Gomez-Llorente, L. Mendez, and A. Riera, J. Phys. B **20**, 6089 (1987).
[15] L. F. Errea, J. M. Gomez-Llorente, L. Mendez, and A. Riera, Phys. Rev. A **35**, 4060 (1987).
[16] T. G. Winter, Phys. Rev. A **37**, 4656 (1988).
[17] L. F. Errea, C. Harel, H. Jouin, J. M. Maidagan, L. Mendez, B. Pons, and A. Riera, Phys. Rev. A **46**, 5617 (1992).
[18] H. Fukuda and T. Ishihara, Phys. Rev. A **46**, 5531 (1992).
[19] P. S. Krstić and R. K. Janev, Phys. Rev. A **47**, 3894 (1993).
[20] K. Runge and D. A. Micha, Phys. Rev. A **53**, 1388 (1996).
[21] G. Hose, Phys. Rev. A **56**, 1364 (1997).
[22] L. F. Errea, C. Harel, C. Illescas, H. Jouin, L. Mendez, B. Pons, and A. Riera, J. Phys. B **31**, 3199 (1998).
[23] C. Harel, H. Jouin, and B. Pons, At. Data Nucl. Data Tables **68**, 279 (1998).
[24] M. E. Riley and B. Ritchie, Phys. Rev. A **59**, 3544 (1999).
[25] C. McCaig and D. S. F. Crothers, J. Phys. B **33**, 3555 (2000).
[26] C. N. Liu, A. T. Le, T. Morishita, B. D. Esry, and C. D. Lin, Phys. Rev. A **67**, 052705 (2003).
[27] P. S. Krstić, J. Phys. B **37**, L217 (2004).
[28] C. D. Lin (private communication); A.-T. Le, C. D. Lin, L. F. Errea, L. Méndez, A. Riera, and B. Pons, Phys. Rev. A **69**, 062703 (2004).
[29] C. C. Havener in *Acceleration-Based Atomic Physics Techniques and Application*, edited by S. M. Shafroth and J. C. Austin (AIP, New York, 1997), p. 117.
[30] P. S. Krstić, C. O. Reinhold, and J. Burgdorfer, Phys. Rev. A **63**, 052702 (2001).
[31] J. S. Thompson, A. M. Covington, P. S. Krstić, Marc Pieksma, J. L. Shinpaugh, P. C. Stancil, and C. C. Havener, Phys. Rev. A **63**, 012717 (2001).
[32] C. C. Havener, M. S. Huq, H. F. Krause, P. A. Schultz, and R. A. Phaneuf, Phys. Rev. A **39**, 1725 (1989).
[33] C. C. Havener, in *The Physics of Multiply and Highly Charged Ions*, edited by Fred J. Currell (Kluwer Academic, Dordrecht, 2003), Vol. 2.
[34] M. Pieksma, M. Gargaud, R. McCarroll, and C. C. Havener, Phys. Rev. A **54**, R13 (1996).

[35] R. E. Olson and M. Kimura, J. Phys. B **15**, 4231 (1982).
[36] C. C. Havener, F. W. Meyer, and R. A. Phaneuf, in *Electronic and Atomic Collisions*, Invited Papers of the XVII International Conference on the Physics of ELectronic and Atomic Collisions, Brisbane, 1991, edited by W. R. MacGillivray, I. E. McCarthy, and M. C. Standage (Institute of Physics, Bristol, 1992), p. 381.
[37] L. R. Andersson, M. Gargaud, and R. McCarroll, J. Phys. B **24**, 2073 (1991).
[38] E. A. Solv'ev, Zh. Eksp. Teor. Fiz. **81**, 1681 (1981) [Sov. Phys. JETP **54**, 893 (1981).]
[39] E. A. Solov'ev, Usp. Fiz. Nauk **157**, 438 (1989) [Sov. Phys. Usp. **32**, 228 (1989)] and references therein.
[40] S. Yu. Ovchinnikov, Phys. Rev. A **42**, 3865 (1990).
[41] P. S. Krstić, D. R. Schultz, and R. K. Janev, J. Phys. B **29**, 1941 (1996).
[42] B. H. Bransden and M. R. C. McDowell, *Charge Exchange and the Theory of Ion-Atom Collisions* (Claredon Press, Oxford, 1992).
[43] T. G. Heil, S. E. Butler, and A. Dalgarno, Phys. Rev. A **23**, 1100 (1981).
[44] B. Johnson, J. Comput. Phys. **3**, 445 (1973).
[45] D. L. Cooper, P. C. Stancil, A. R. Turner, J. G. Wang, N. J. Clarke, and B. Zygelman, Int. J. Mol. Sci. **3**, 220 (2002).
[46] R. Hoekstra, F. J. de Heer, and R. J. Morgenstern, J. Phys. B **24**, 4025 (1991).
[47] G. W. McClure, Phys. Rev. **148**, 47 (1966).
[48] R. J. Mawhorter, J. Greenwood, S. J. Smith, and A. Chutjian, in *Proceeding of the 35th Meeting of the APS, Division of Atomic, Molecular and Optical Physics, Tucson, Arizona, 2004* [Bull. Am. Phys. Soc. 49, J1.019 (2004).]
[49] D. Čirič, D. Dijkkamp, E. Vlieg, and F. J. de Heer, J. Phys. B **18**, 4745 (1985).
[50] D. Čirič, R. Hoekstra, F. J. de Heer, and R. Morgenstern, in *Electronic and Atomic Collisions*, edited by H. B. Gilbody, W. R. Newell, F. H. Read, and A. C. H. Smith (North-Holland, Amsterdam, 1988), p. 655.